

How does geometry affect quantum gases?

A. A. Araújo Filho^{1,*} and J. A. A. S. Reis^{2,3,†}

¹*Universidade Federal do Ceará (UFC), Departamento de Física,
Campus do Pici, Fortaleza - CE, C.P. 6030, 60455-760 - Brazil.*

²*Universidade Federal do Maranhão (UFMA), Departamento de Física,
Campus Universitário do Bacanga, São Luís - MA, 65080-805, Brazil*

³*Universidade Estadual do Maranhão (UEMA), Departamento de Física,
Cidade Universitária Paulo VI, São Luís - MA, 65055-310, Brazil*

(Dated: April 8, 2022)

Abstract

In this work, we study the impact of different *non-Cartesian* geometries (spherical, cylindrical, ellipsoidal and toroidal ones) on the thermodynamic functions of quantum gases. We start with the simplest situation, namely, spinless gas treated within the canonical ensemble framework. As a next step, we consider *non-interacting* gases (fermions and bosons) with the usage of the grand canonical ensemble description. For this case, the calculations are performed numerically and we illustrate our results addressing two possible applications: *Bose-Einstein condensate* and *helium dimer*. Moreover, the bosonic sector, independently of the geometry, acquires entropy and internal energy greater than fermionic case. Another notable aspect is present as well: the thermal properties turn out to be sensitive to the topological parameter (winding number) for the toroidal case. Finally, we also devise a model allowing to perform analytically the calculations in the case of *interacting* quantum gases, and, afterwards, we apply it to three different cases: cubical box, ring and torus.

*Electronic address: dilto@fisica.ufc.br

†Electronic address: jalfieres@gmail.com

I. INTRODUCTION

The investigation of thermal aspects of materials has gained considerable attention in recent years especially in the context of condensed matter physics and the development of new materials [1–4]. Given the existence of some well-known approximations, the electrons of a metal can be assumed to be a gas due to their free moving behavior [5–10]. Such studies are worth exploring due to their relevance in fundamental [11, 12] and applied [13, 14] physical contexts. In parallel, a longstanding issue in quantum mesoscopic systems is the methods to perform an exact sum over the states of either *interacting* or *non-interacting* particles. Depending on the situation, the boundary effects cannot be neglected, instead, they should be taken into account in order to acquire a better correlation with the experimental results. Moreover, the properties of some systems are assumed to be shape dependent [15–17] and sensitive to their topology [18–22].

From a theoretical viewpoint, a related problem of statistical mechanics is performing the sum over all accessible quantum states to obtain the physical quantities [23, 24]. Normally, the spectrum of particle states, which are confined in a volume, will be elucidated by the study of boundary effects. Nevertheless, if the particle wavelength is too short in comparison with the characteristic scale of the respective occupation system, the boundary effect can be overlooked. In previous years, such an assumption was supported by Rayleigh and Jeans in their radiation theory of electromagnetism [25]. Furthermore, such an involvement also emerged in a purely mathematical context and was rigorously solved afterwards by Hermann Weyl [26].

Based on aforementioned novelties highlighted thus, this work aims at studying how the thermodynamic functions of quantum gases behave within different *non-Cartesian* geometries, i.e., spherical, cylindrical, ellipsoidal and toroidal ones. Additionally, for the sake of their experimental test, we employ a toy model to accomplish such calculations for both *non-interacting* and *interacting* particle modes. Therefore, our results might serve as a basis for practical applications, and might help to nuance an emerging phenomena concerning further promising studies in condensed matter physics and statistical mechanics.

Initially, in Section II, we present a discussion involving the spectral energy for different geometries. After, in Section III, we focus on spinless particles using the theory of canonical ensemble. Next, in Section IV, we focus on *non-interacting* gases (fermions and bosons)

within the same geometries with the usage of the grand-canonical ensemble though. Moreover, in Section VI, we propose two applications towards such a direction: *Bose-Einstein condensate* and *helium dimer*. Next, in Section VII, we devise a model to perform the calculations of *interacting* quantum gases which is applied to three different cases: cubical box, ring and torus. These latter three turn out to be more prominent since all the results were derived analytically. Finally, in Section VIII, we make our final remarks, conclusions and future perspectives.

II. SPECTRAL ENERGY FOR DIFFERENT GEOMETRIES

Initially, we study the thermodynamic properties of confined gases: spinless ones, fermions and bosons with a non-trivial spin. To do that, we must solve the Schrödinger equation for particular symmetries with appropriate boundary conditions. With this, the spectral energy can be derived after some algebraic manipulations. In particular, we choose four 3-dimensional geometries, namely, spherical, cylindrical, ellipsoidal and toroidal ones. The potentials for each configuration are given in the equations below:

$$\mathcal{V}_{\text{Sphere}}(r) = \begin{cases} 0, & \text{if } r < a \\ \infty, & \text{if } r > a \end{cases}, \quad (1)$$

$$\mathcal{V}_{\text{Cylinder}}(r) = \begin{cases} 0, & \text{if } \rho < b \text{ and } 0 < z < 2c \\ \infty, & \text{otherwise} \end{cases}, \quad (2)$$

$$\mathcal{V}_{\text{Ellipsoid}}(r) = \begin{cases} 0, & \text{if } x, y, z \text{ satisfy } \frac{x^2+y^2}{b^2} + \frac{z^2}{c^2} < 1 \\ \infty, & \text{if } x, y, z \text{ satisfy } \frac{x^2+y^2}{b^2} + \frac{z^2}{c^2} \geq 1 \end{cases}, \quad (3)$$

and

$$\mathcal{V}_{\text{Torus}}(r) = \begin{cases} 0, & \text{if } (\sqrt{x^2 + y^2 - R})^2 + z^2 < r^2 \\ \infty, & \text{otherwise} \end{cases}. \quad (4)$$

where a , b and c are geometric parameters defining the size of the potential, and R is the distance from the center of the tube to the center of the torus. In order to make a comparison between our thermodynamic results in the next sections, we must choose the parameters a , b and c such that all potentials have the same volume. Since we have already set up our potentials, we can solve the time-independent Schrödinger equation

$$-\frac{\hbar^2}{2m} \nabla^2 \psi + V(r) \psi = E \psi, \quad (5)$$

for each geometry whose solutions can be obtained using the well-known method of separation of variables [25, 27–29]. Particularly, the wave function for the spherical case can be written as

$$\psi(r) = \begin{cases} A_l j_l(r) Y_l^m, & \text{if } r \leq a \\ 0, & \text{if } r \geq a \end{cases}, \quad (6)$$

where $j_l(r)$ is the spherical Bessel function, Y_l^m is the spherical harmonic and A_l is the normalization factor; thereby, the Fourier transform of ψ is

$$\tilde{\psi}(k) = \frac{1}{\sqrt{(2\pi\hbar)^3}} A_l \int_0^a e^{ik \cdot r} j_l(r) Y_l^m(r') r^2 dr dr' \quad (7)$$

and using the orthogonality properties of the Bessel functions [30–32], we can infer about the momentum distribution $n(k)$

$$n(k) = \frac{12sV}{\pi^2(\pi\hbar)^3} \sum (2l+1) j_l^2(ka) \frac{(k_l a/\pi)^2}{[(k_l a/\pi)^2 - (ka/\pi)^2]^2}, \quad (8)$$

where s is the spin degeneracy. In Ref. [33], some approximations in order to derive analytical and numerical analysis of *non-interacting* particles at zero temperature were made. The shape dependence was investigated as well to see how such geometries would influence the momentum distribution $n(k)$. Our approach, on the other hand, intends to examine the impact of *non-Cartesian geometries* on the thermodynamic properties differing to the results encountered in the literature [16, 17]. For doing so, we consider spherical, cylindrical, ellipsoidal and toroidal configurations to perform the following calculations. Solving the Schrödinger equation for the spherical potential, we have

$$E_{n,l}^{\text{Sphere}} = (2l+1) \frac{\hbar^2}{2ma^2} j_{nl}^2. \quad (9)$$

where j_{nl} is the n th zero of the l th spherical Bessel function. Clearly, each level has $(2l+1)$ degeneracy. For ellipsoidal, cylindrical and toroidal shapes, we obtain

$$E_{m,n,l}^{\text{Ellipsoid}} = \frac{\hbar^2}{2m} \left[\frac{J_{n,l}^2}{b^2} + \frac{2J_{n,l}}{bc} \left(m + \frac{1}{2} \right) \right], \quad (10)$$

$$E_{m,n,l}^{\text{Cylinder}} = \frac{\hbar^2}{2m} \left[\frac{J_{n,l}^2}{b^2} + \left(\frac{\pi m}{2c} \right)^2 \right], \quad (11)$$

and

$$E_n^{\text{Torus}} = \frac{n^2}{2ma^2p^2} \frac{\cosh^2 \eta}{\alpha^2 + \sinh^2 \eta - 1}, \quad (12)$$

where $J_{n,l}$ is the n th zero of the l th Bessel function of the first kind, η is a parameter which fixes the toroidal surface, α is the winding number, a and p are parameters ascribed to the torus shape and $m = 0, 1, \dots$. With use of these spectra, the thermal analysis can be properly derived in the next sections.

III. NON-INTERACTING GASES: SPINLESS PARTICLES

In this section, it is enough to present the thermodynamic method based on the canonical ensemble.

A. Thermodynamic approach

Whenever we are dealing with a spinless gas, the theory of canonical ensemble is sufficient for a full thermodynamical description. Thereby, the partition function is given by

$$\mathcal{Z} = \sum_{\{\Omega\}} \exp(-\beta E_{\Omega}), \quad (13)$$

where Ω is related to accessible quantum states. Since we are dealing with *non-interacting* particles, the partition function (13) can be factorized which gives rise to the result below

$$\mathcal{Z} = \mathcal{Z}_1^N = \left\{ \sum_{\{\Omega\}} \exp(-\beta E_{\Omega}) \right\}^N, \quad (14)$$

where we have defined the single partition function as

$$\mathcal{Z}_1 = \sum_{\Omega} \exp(-\beta E_{\Omega}). \quad (15)$$

As it is known, the thermodynamical description of the system can also be done via Helmholtz free energy

$$f = -\frac{1}{\beta} \lim_{N \rightarrow \infty} \frac{1}{N} \ln \mathcal{Z}, \quad (16)$$

where rather for convenience we write the Helmholtz free energy per particle. With this, we can derive the following thermodynamic state functions¹, i.e., entropy, heat capacity and mean energy

$$s = -\frac{\partial f}{\partial T}, \quad (17)$$

¹ All of them are written in a “per particle form” for convenience.

$$c = T \frac{\partial s}{\partial T}, \quad (18)$$

and

$$u = -\frac{\partial}{\partial \beta} \ln \mathcal{Z}. \quad (19)$$

The sum in Eq. (15) cannot be expressed in a closed form. This does not allow us to proceed analytically. To overcome this situation, we perform a numerical analysis plotting the respective graphics in order to understand such behaviors. Our main interest lies in the study of low temperature regime. In this case, we need to take into account many terms in the sum (15). We also need to point out that the thermodynamic limit is not taken in an usual way, since we are keeping the volume V constant.

B. Numerical analysis

To provide the numerical results below, we sum over about fifty thousand terms in the Eq. (15). With this, we can guarantee the accuracy of such procedure keeping the maximum of details. For the plots below, we choose the following values for the parameters a , b and c that control the size of potential: $a = 1.0$, $b = 1.0$ and $c = 0.66$ (thick lines) and $a = 1.5$, $b = 1.22$ and $c = 1.5$ (dashed lines). For now on, we will refer to the configuration 1 and the configuration 2 respectively. We must remember that those parameters are chosen such that all the infinite wells have the same volume. The graphics for the configurations described are displayed below in Fig. 1 and Fig. 2.

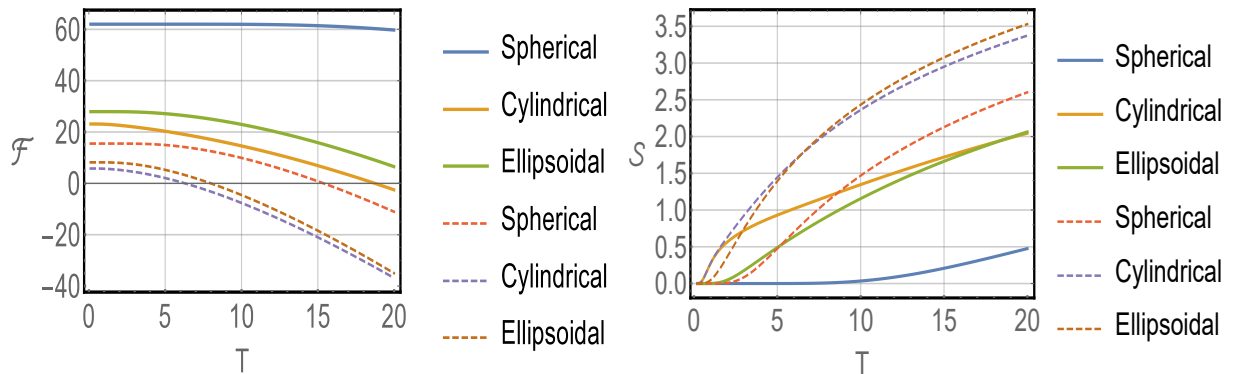


Figure 1: Here we display the Helmholtz free energy and entropy per particle.

Let us start analyzing the free energy. In Fig. 1, we see that the configuration 1 provides a free energy greater than the configuration 2. Besides, we also see that energy increases as

Sphere > *Ellipsoid* > *Cylinder* in both configurations. The behavior for the entropy, on the other hand, seems to be different. We notice that the configuration 2 provides an entropy greater than the configuration 1 and, when we look at the geometry itself, it follows the pattern *Cylinder* > *Ellipsoid* > *Sphere*. In this comparison, the *Ellipsoidal* geometry always occupies a middle position. This fact is rather natural since this geometry is actually a “transition” between a cylinder and a sphere.

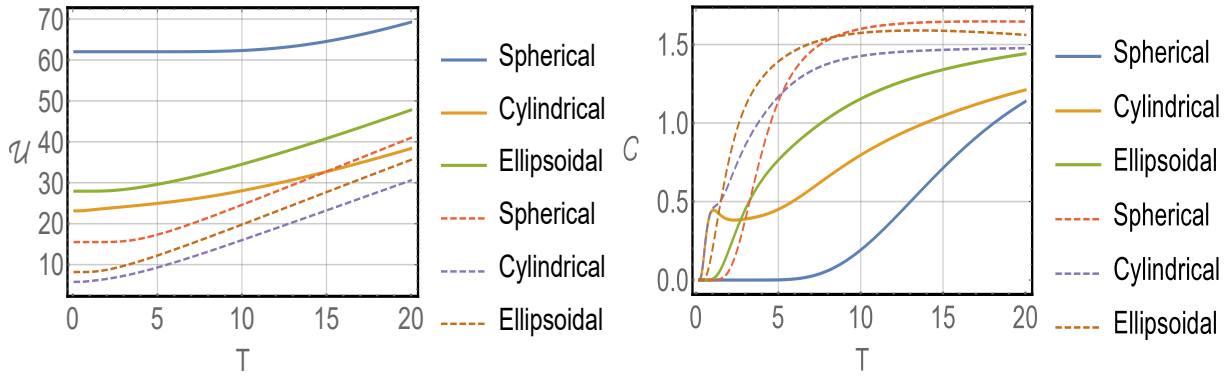


Figure 2: Here we display the internal energy and heat capacity per particle.

In Fig. 2, we find the plots for the internal energy and for the heat capacity. The configuration 1 shows its energy greater than configuration 2 and follows from the plots which are independent of the configuration; and we see that the internal energy increases as *Sphere* > *Ellipsoid* > *Cylinder*. The heat capacities for all configurations approach the value $3/2$ as temperature increases. The configuration 2, that has a larger volume, reaches asymptotic value faster than configuration 1. Differently from what we saw for the other thermodynamic quantities, it is not possible to establish a common behavior of *Ellipsoid*, *Cylinder* and *Sphere* geometries because of different temperature ranges and well sizes (they vary drastically their values). For instance, in configuration 2 in the range $0 < T < 5 k$, we see that the heat capacity follows the rule *Ellipsoid* > *Cylinder* > *Sphere*. However, in the same range of temperature, the configuration 1 displays two different behaviors, that is for $0 < T < 2.5 k$ we have *Cylinder* > *Ellipsoid* > *Sphere* and for $2.5 < T < 5 k$ we have *Ellipsoid* > *Cylinder* > *Sphere*. For a fixed value of volume, there exists a temperature where the heat capacity will follow the rule *Sphere* > *Ellipsoid* > *Cylinder* until it reaches the value $3/2$. This temperature increases as the volume decreases in the configuration 1 the temperatures where we have this order is around $29k$ and for configuration 2, that has

a larger volume, it happens at $9k$. It is interesting to see that for the cylindrical geometry a slop appears around $0.5k$ and tends to disappear when the volume of the cylinder increases. This effect is clearly caused by the finite size of the geometry since the expected behavior would be to go to zero almost linearly. However, both sphere and the ellipsoid do not present such effect. We could conclude about the absence of such effect that the former cases accentuates those geometries are smooth from the point of view of the surface and for the cylinder, on the other hand, the surface considered is smooth just by parts. As we will see in Sec. VII and in Ref. [17], it is possible to identify the contribution that comes from the geometry itself when we considered an analytical model.

IV. NON-INTERACTING GASES: BOSONS AND FERMIONS

Although interactions of atoms and molecules are treated in many experimental approaches, and several features may only be recognized and understood by taking the interactions into account [34–37], some fascinating characteristics are well described by assuming *non-interacting* systems [38–50].

Studies of *non-interacting* particles (bosons and fermions) have many applications, especially in chemistry [48, 49] and condensed matter physics [38–47, 50, 51]; for instance, in the case of *bulk*, which is usually assumed to calculate the energy spectrum and use the *Fermi-Dirac* distribution to examine how its statistics behave, it is sufficient to describe the system of *non-interacting* electron gas. Such assumption is totally reasonable since if the *Fermi energy* is large enough, the kinetic energy of electrons, close to the Fermi level, will be much greater than the potential energy of *electron-electron* interaction.

On the other hand, one of the pioneer studies which addressed the analysis of the *Bose-Einstein condensate* in a theoretical view point was presented in [52]. The authors utilize a gas of *non-interacting* bosons to perform their calculations. As we shall see, we proceed in a similar way taking into account different geometries though. Furthermore, we discuss applying them in different scenarios in condensed matter physics.

A. Thermodynamic approach

We intend to apply the grand canonical ensemble theory for N *non-interacting* particles with different spins (fermions and bosons); we will treat both cases separately. The grand canonical partition function for the present problem reads

$$\Xi = \sum_{N=0}^{\infty} \exp(\beta\mu N) \mathcal{Z}[N_{\Omega}], \quad (20)$$

where $\mathcal{Z}[N_{\Omega}]$ is the usual canonical partition function which now depends on the occupation number N_{Ω} . Since we are dealing with fermions and bosons, it is well known that the occupation number must be restricted in the following manner: $N_{\Omega} = \{0, 1\}$ for fermions and $N_{\Omega} = \{0, \dots, \infty\}$ for bosons. Also, for an arbitrary quantum state, the energy depends on the occupation number as

$$E\{N_{\Omega}\} = \sum_{\{\Omega\}} N_{\Omega} E_{\Omega}$$

where we have

$$\sum_{\{\Omega\}} N_{\Omega} = N.$$

In this way, the partition function becomes

$$\mathcal{Z}[N_{\Omega}] = \sum_{\{N_{\Omega}\}} \exp \left[-\beta \sum_{\{\Omega\}} N_{\Omega} E_{\Omega} \right], \quad (21)$$

which leads to

$$\Xi = \sum_{N=0}^{\infty} \exp(\beta\mu N) \sum_{\{N_{\Omega}\}} \exp \left[-\beta \sum_{\{\Omega\}} N_{\Omega} E_{\Omega} \right], \quad (22)$$

or can be rewritten as

$$\Xi = \prod_{\{\Omega\}} \left\{ \sum_{\{N_{\Omega}\}} \exp[-\beta N_{\Omega} (E_{\Omega} - \mu)] \right\}. \quad (23)$$

After performing the sum over the possible occupation numbers, we get

$$\Xi = \prod_{\{\Omega\}} \{1 + \chi \exp[-\beta (E_{\Omega} - \mu)]\}^{\chi}, \quad (24)$$

where we have now introduced the convenient notation $\chi = +1$ for fermions and $\chi = -1$ for bosons. The connection with thermodynamics is made by using the grand thermodynamical potential given by

$$\Phi = -\frac{1}{\beta} \ln \Xi. \quad (25)$$

Replacing Ξ in the above equation, we get

$$\Phi = -\frac{\chi}{\beta} \sum_{\{\Omega\}} \ln \{1 + \chi \exp [-\beta (E_\Omega - \mu)]\}. \quad (26)$$

The entropy of the system can be cast in the following compact form, namely

$$S = -\frac{\partial \Phi}{\partial T} = -k_B \sum_{\{\Omega\}} \mathcal{N}_\Omega \ln \mathcal{N}_\Omega + \chi (1 - \chi \mathcal{N}_\Omega) \ln (1 - \chi \mathcal{N}_\Omega)$$

where

$$\mathcal{N}_\Omega = \frac{1}{\exp [\beta (E_\Omega - \mu)] + \chi}.$$

Moreover, we can also use the grand potential to calculate other thermodynamic properties, such as, mean particle number, energy, heat capacity and pressure using the following expressions:

$$\mathcal{N} = -\frac{\partial \Phi}{\partial \mu}, \quad (27)$$

$$\mathcal{U} = -T^2 \frac{\partial}{\partial T} \left(\frac{\Phi}{T} \right), \quad (28)$$

$$C = T \frac{\partial S}{\partial T}, \quad (29)$$

$$\mathcal{P} = -\frac{\partial \Phi}{\partial V} = -\frac{\Phi}{V}. \quad (30)$$

In possession of these terms, calculating the thermodynamic quantities should be a straightforward task, since one only would need to perform the sum presented in Eq. (26). Unfortunately, this sum cannot be obtained in a closed form for the spectral energy that we chose. Instead of this, a numerical analysis, similar to what we have done in Sec. III B, can be provided to overcome this difficulty; thereby, we can obtain the behavior of all quantities considering mainly low temperature regimes (keeping the volume constant). In what follows, we devote our attention to study such properties in a numerical form.

B. Numerical analysis

Here, as in previous numerical analyses, we consider two particular cases for different values: $a = 1.0, b = 1, 0$ and $c = 0, 66$ (referred as case 1); and $a = 1.5, b = 1, 22$ and $c = 1, 5$ (as case 2). Next, we also use thick and dashed lines to represent fermions and bosons in the plots presented in Figs. 3, 4 and 5. In Fig. 3, we present the entropy for the two different

cases. The first one, in Fig. 3a, represents the case 1 and Fig. 3b the case 1, where we compare fermions (thick lines) and bosons (dashed lines) for all geometries we proposed. We can see from the plots that bosons, independently of the geometry, acquire an entropy great than fermions. We can also realize that the pattern *Ellipsoid* > *Cylinder* > *Sphere* always occur for fermions and bosons when we consider the entropy. In both cases the pattern described above repeats and shows that the entropy is a monotonically increasing function for the volume and temperature.

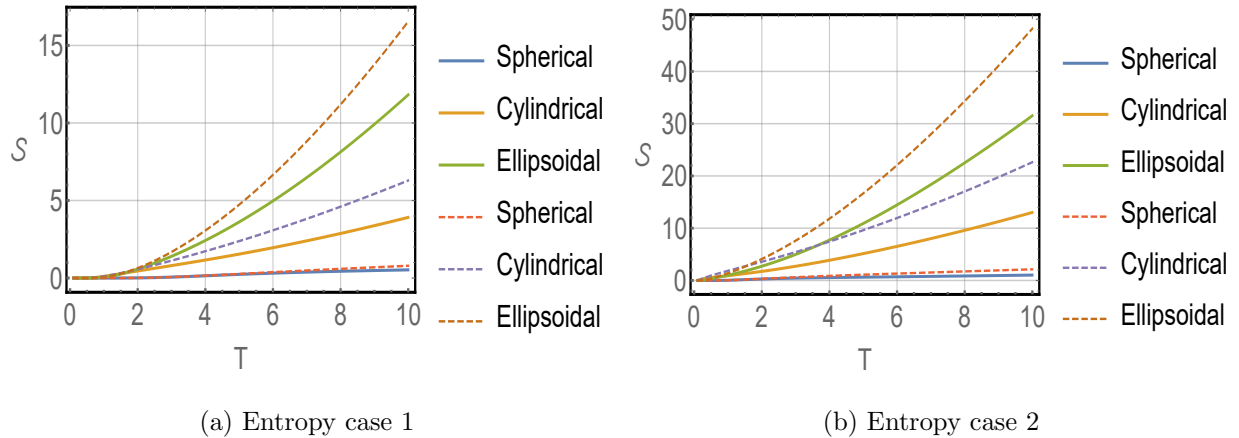


Figure 3: The different behaviors for the entropy.

For the internal energy, plotted in Fig. 4, we see the entire behavior being repeated, that is, the internal energy follows the rule *Ellipsoid* > *Cylinder* > *Sphere* and the energy for the bosons are greater than fermions when we compare their values for the same geometry. It is also important to notice that the internal energy is a monotonically increasing function for both volume and temperature.

Another important property analyzed here is the heat capacity, plotted in Fig. 5. We know from literature [23, 24] that the heat capacity for an electron gas at a low temperature ($T \ll T_{Fermi}$) is proportional to the temperature and the gas of bosons, on the other hand, is proportional to $T^{3/2}$ (both behaviors are obtained in the classical limit). However, as we can note from the graphics, in both cases presented in Fig. 5, the fermions do not follow this rule. We see deviation from a straight line (for fermions), where one can infer that this effect is caused by the finite volume. On the other hand, the bosons behave exactly like a function proportional to $T^{3/2}$. It suggests that fermions are more sensitive to the geometry and size than bosons. Besides the discussion above, we can also see that in general the heat

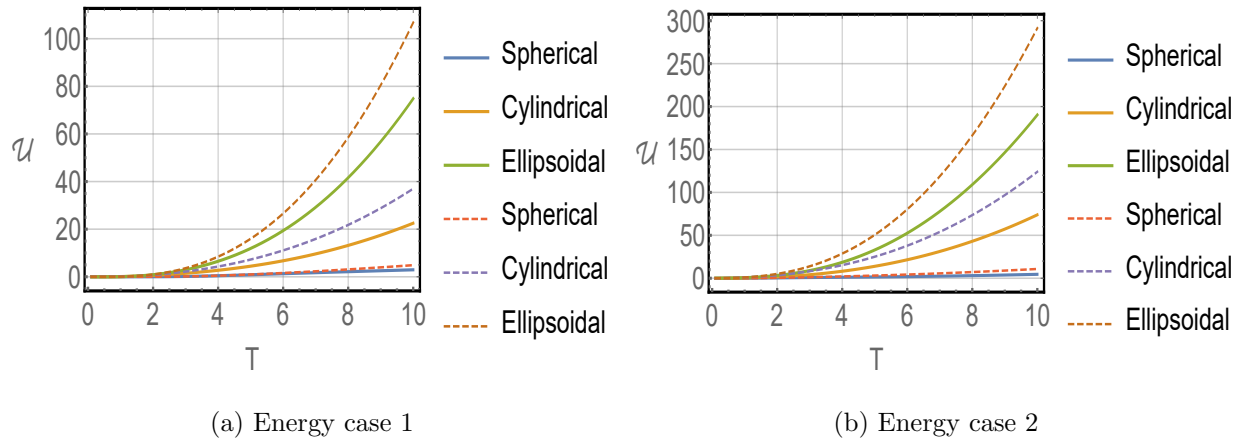


Figure 4: The different behaviors for the mean energy.

capacity follows the pattern *Ellipsoid* > *Cylinder* > *Sphere* and its value increases when both temperature and volume increase.

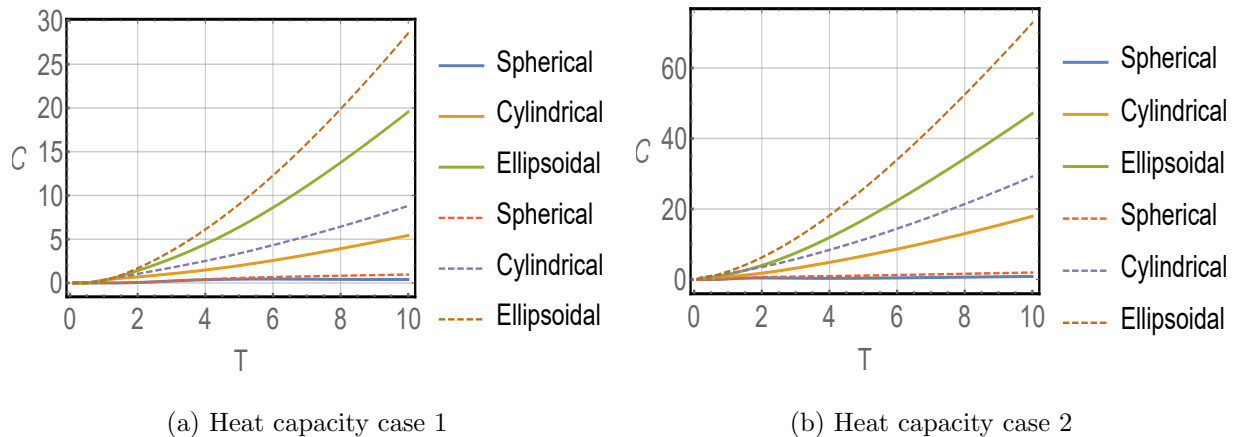


Figure 5: The different behaviors for the heat capacity.

V. IDEAL QUANTUM GAS ON A TORUS KNOT

In the last years, the study of quantum mechanics in constrained systems has gained much attention acquiring diverse applications in both theoretical and experimental approaches [53–62]. It was Jones [63] who examined knot invariants to address the connection between physical world and rigorously pure mathematics. Afterwards, such approach was linked to topological quantum field theory by Witten [64, 65]. It is worth mentioning that the

connection of such invariant knots with statistical mechanics is also possible [66]. Another motivation to investigate the physical consequences of the torus topology ($T^2 = S^1 \times S^1$) is its application to living beings, owing their DNA [67–71]. Moreover, the fundamental group of the torus is

$$\pi_1(T^2) = \pi_1(S^1) \times \pi_1(S^1) \cong \mathbb{Z}^1 \times \mathbb{Z}^1, \quad (31)$$

and its first homology group is isomorphic to the fundamental group [72]. Now, based on Ref. [60], where the spectral energy for the torus knot was calculate, and in the approach developed in Sec. III and Sec. IV, we purpose the study how different spin particles behave in such a scenario. Before providing numerical analyses, let us show again the spectral energy [60] as in Eq. (12)

$$E_n = E_{0,n} F(\eta, \alpha),$$

where

$$E_{0,n} = \frac{n^2}{2ma^2p^2}, \quad F(\eta, \alpha) = \frac{\cosh^2 \eta}{\alpha^2 + \sinh^2 \eta - 1}.$$

Now we can insert the energy spectrum in Eqs. (14) and (26) and perform properly the following numerical analyses for both energy and heat capacity. We first study the energy behavior presented in Fig. 6. We can see that fermions and bosons behave differently. While bosons increase with temperature and winding number, the fermions have an “inversion point” at $3k$, e.g., before and after $3k$ there exist different behaviors for diverse values of winding numbers. Moreover, for spin-less particles the Helmholtz free energy decreases with both temperature and winding number.

In Fig. 7, we present the heat capacity for different particle spins and different values of the winding numbers. Let us start with the spin-less particles. In this case, we see that the heat capacity increases with the winding number and tends to $0.5 J/g \times k$ for larger values of temperature. For bosons, we see that for temperature below $0.3k$, the values of heat capacity decreases when the winding number increases, while for temperatures above $0.3k$ the values increases when α increases. It is worth mentioning that for large values of temperature, the heat capacity tends to $8.0 J/g \times k$. Finally, we observe an interesting behavior for fermions. We see that for temperatures below $1.0k$ the heat capacity has a slope that becomes more evident when the winding number increases. Above $1.0k$ the heat capacity increases with temperature until reach a value around $2.0 J/g \times k$. It is interesting to see a system that has its thermodynamic properties being modified by a topological parameter. Thereby, the

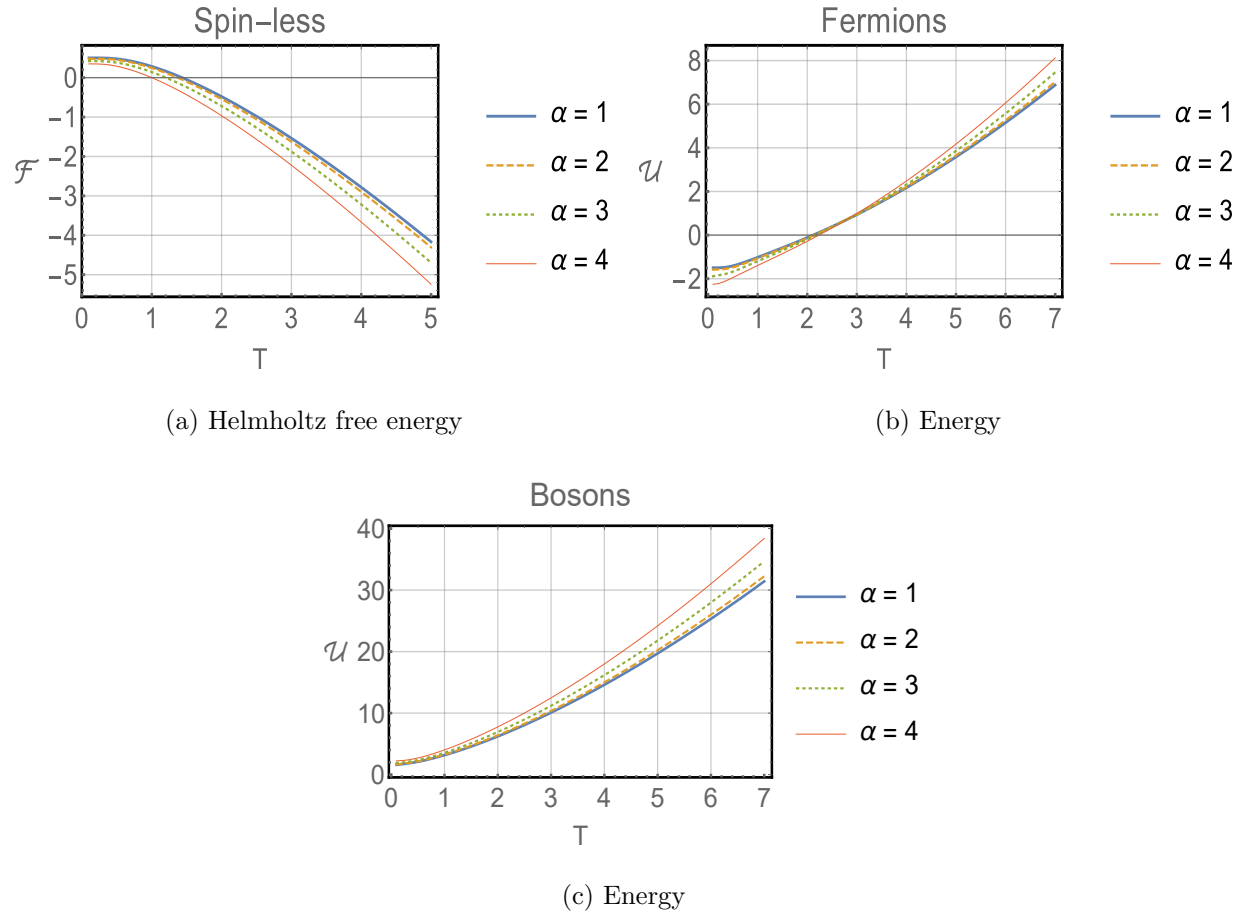


Figure 6: Energy behavior for low temperature regime for different values of winding number α for the torus knot.

knowledge of such behaviors can be useful for future applications.

VI. FURTHER APPLICATIONS: NON-INTERACTING GASES

In this section, we address possible future applications of our *non-interacting* model for quantum gases developed so far; in particular, we look toward *Bose-Einstein condensate* and *helium dimer*.

A. Bose-Einstein condensate

In Ref. [52], the grand canonical ensemble is also used to perform the calculations; the authors studied the asymptotic behavior of various thermodynamic and statistical quantities

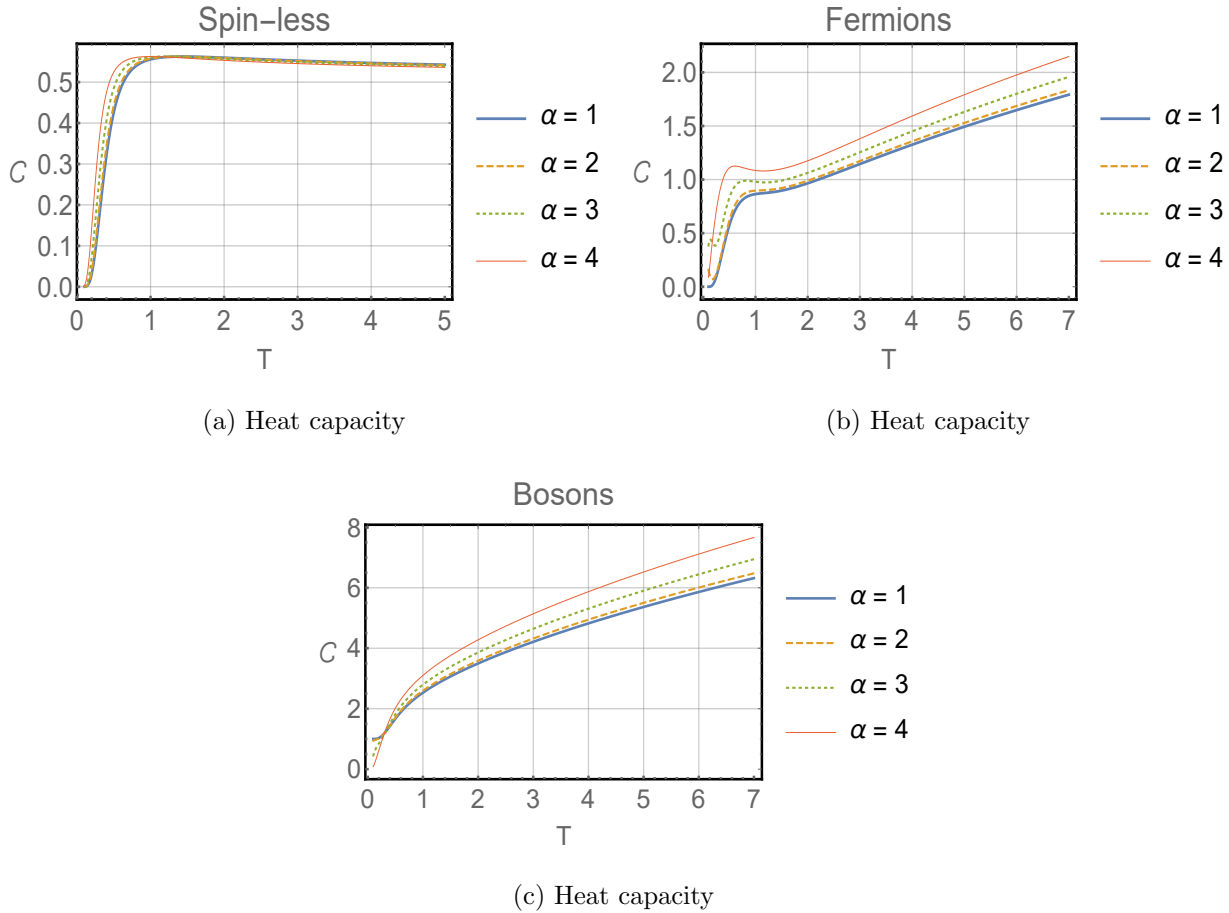


Figure 7: Heat capacity for low temperature regime for different values of winding number α for the torus knot.

related to a confined ideal *Bose-Einstein* gas. In this case, the considered object is an arbitrary, finite, cuboidal enclosure subjected to periodic boundary conditions, i.e., thin-film, square-channel and cubic geometries.

Continuing the line of [52], our proposition is to probe how the thermal quantities are affected by spherical, cylindrical, ellipsoidal and toroidal geometries. This study can be useful within a possible future experimental scenario to be studied in material science.

B. Helium atoms - 3He and 4He

Taking the advantage of solving the Schrödinger equation numerically as well as the construction of suitable wave functions, in Refs. [73, 74], the binding of two helium atoms

involving restricted and unrestricted geometries was studied for two and three dimensions. Such model regards two atoms placed in a spherical potential (1) with hard walls. As argued, one could insert a non-trivial interaction of the helium atoms with the walls [75–78] and also some coupling between them, as presented in Sec. VII. Nevertheless, interaction of the particles with the wall depends on the material of the cavity. Thereby, it is feasible to propose a general investigation of these phenomena than be rather limited for individual cases.

In this sense, our proposal is as follows: based on the relevance of studying either the helium liquids or helium dimer in solid matrices, the study how geometry influences the thermodynamic properties of such constrained systems might be relevant for future applications in condensed matter physics. Likewise, for the cylindrical shape (2), it is notable to aim at investigating the thermal properties of a carbon-like shape nanotubes [79, 80]. Also, using some approximations, the vortex-like shapes [81, 82] seem to reasonable to be examined as well.

VII. INTERACTING GASES: AN ANALYTICAL APPROACH

A. The model

We intend now to take into account interactions between particles. To do so, we modify slightly the approach developed in Sec. IV by introducing a interaction term $U(V, n)$. Throughout this section, we adopt natural units here $k_B = 1$. Doing that, we get the following grand canonical partition function

$$\mathcal{Z}(T, V, \mu) = \sum_{\{N_\Omega\}=0}^{\{\infty/1\}} \exp \left\{ -\beta \left[\sum_{\{\Omega\}} N_\Omega (E_\Omega - \mu) + U(V, n) \right] \right\}, \quad (32)$$

where

$$z^N = \exp \{N\beta\mu\} = \exp \left\{ \beta \sum_{\{\Omega\}} N_\Omega \mu \right\}.$$

It is worth mentioning that our approach can be used for both *Cartesian* and *non-Cartesian* geometries, so that we can explore a variety of cases as long as there a discrete spectral energy is present. The sum index which appears in Eq. (32), namely $\{\infty/1\}$, shows that, in the same quantum state Ω , infinitely many bosons may be added. On the other hand, if

one considers instead of this, spin-half particles, only one fermion is allowed due to the Pauli exclusion principle. In a compact notation, we take the upper index ∞ for bosons and 1 for fermions. Let us suppose that the interaction term is $U(V, n) = Vu(n)$, where $n = N/V$ is the so-called particle density. Thereby, we have

$$\mathcal{Z}(T, V, \mu) = \sum_{\{N_\Omega\}=0}^{\{\infty/1\}} \exp \left\{ -\beta \left[\sum_{\{\Omega\}} N_\Omega (E_\Omega - \mu) + Vu(n) \right] \right\}. \quad (33)$$

For the sake of simplicity, within the expression (33), we assume that $Vu(n)$ is linear in $\sum_\Omega N_\Omega = N$. Furthermore, the only appropriate manner to do that consists in linearizing $Vu(n)$. To do that, we use the Taylor series expansion of $u(n)$ around the mean value \bar{n} :

$$u(n) = u(\bar{n}) + u'(\bar{n})(n - \bar{n}) + \dots \quad (34)$$

It follows that energy of the quantum state Ω is

$$E = \sum_{\{\Omega\}} N_\Omega E_\Omega + \sum_{\{\Omega\}} N_\Omega u'(\bar{n}) + U(V, \bar{n}) - u'(\bar{n}) \bar{N}. \quad (35)$$

With it, the solution of Eq. (33) can be evaluated

$$\begin{aligned} \mathcal{Z}(T, V, \mu) &= \exp \left\{ -\beta [U(V, \bar{n}) - u'(\bar{n}) \bar{N}] \right\} \\ &\times \prod_{\Omega=1}^{\infty} \left(\sum_{N_\Omega=0}^{\{\infty/1\}} \exp \left\{ -\beta [E_\Omega + u'(\bar{n}) - \mu] N_\Omega \right\} \right). \end{aligned} \quad (36)$$

After some algebraic manipulations, we can present the above expression as

$$\begin{aligned} \mathcal{Z}(T, V, \mu) &= \exp \left\{ -\beta [U(V, \bar{n}) - u'(\bar{n}) \bar{N}] \right\} \\ &\times \prod_{\Omega=1}^{\infty} \begin{cases} 1 + \exp [-\beta (E_\Omega + u'(\bar{n}) - \mu)], \text{ fermions} \\ (1 - \exp [-\beta (E_\Omega + u'(\bar{n}) - \mu)])^{-1}, \text{ bosons} \end{cases}, \end{aligned} \quad (37)$$

or in a more compact form

$$\begin{aligned} \mathcal{Z}(T, V, \mu) &= \exp \left\{ -\beta [U(V, \bar{n}) - u'(\bar{n}) \bar{N}] \right\} \\ &\times \prod_{\Omega=1}^{\infty} (1 + \chi \exp [-\beta (E_\Omega + u'(\bar{n}) - \mu)])^\chi, \end{aligned} \quad (38)$$

where $\chi = 1$ for fermions, and $\chi = -1$ for bosons.

B. Thermodynamic state quantities

Next, the derivation of the grand canonical potential is straightforward as follows

$$\begin{aligned}\Phi &= -T \ln \mathcal{Z} \\ &= -T \chi \sum_{\Omega} \ln (1 + \chi \exp [-\beta (E_{\Omega} + u'(\bar{n}) - \mu)]) + U(V, \bar{n}) - u'(\bar{n}) \bar{N}.\end{aligned}\quad (39)$$

Based on this equation, the other thermodynamic functions can be calculated as well. In this sense, the mean particle number reads

$$\begin{aligned}\bar{N} &= - \frac{\partial \Phi}{\partial \mu} \Big|_{T,V}, \\ &= -V \frac{\partial u(\bar{n})}{\partial \mu} \Big|_{T,V} + \bar{N} \frac{\partial u'(\bar{n})}{\partial \mu} \Big|_{T,V} + u'(\bar{n}) \frac{\partial \bar{N}}{\partial \mu} \Big|_{T,V} + \\ &\quad + T \chi \sum_{\Omega} \frac{\chi \exp [-\beta (E_{\Omega} + u'(\bar{n}) - \mu)]}{1 + \chi \exp [-\beta (E_{\Omega} + u'(\bar{n}) - \mu)]} \beta \left(1 - \frac{\partial u'(\bar{n})}{\partial \mu} \Big|_{T,V} \right),\end{aligned}\quad (40)$$

and from this,

$$\begin{aligned}\bar{N} \left(1 - \frac{\partial u(\bar{n})}{\partial \mu} \Big|_{T,V} \right) &= -V \frac{\partial u(\bar{n})}{\partial \mu} \Big|_{T,V} + u'(\bar{n}) \frac{\partial \bar{N}}{\partial \mu} \Big|_{T,V} \\ &\quad + \chi^2 \beta T \left(1 - \frac{\partial u'(\bar{n})}{\partial \mu} \Big|_{T,V} \right) \sum_{\Omega} \frac{1}{\exp [\beta (E_{\Omega} + u'(\bar{n}) - \mu)] + \chi}.\end{aligned}\quad (41)$$

Since

$$\frac{\partial u(\bar{n})}{\partial \mu} \Big|_{T,V} = u'(\bar{n}) \frac{\partial \bar{n}}{\partial \mu} \Big|_{T,V} = \frac{u'(\bar{n})}{V} \frac{\partial \bar{N}}{\partial \mu} \Big|_{T,V},\quad (42)$$

we get

$$\bar{N} = \sum_{\Omega} \frac{1}{\exp [\beta (E_{\Omega} + u'(\bar{n}) - \mu)] + \chi},\quad (43)$$

the mean occupation number must be $\bar{N} = \sum_{\Omega} \bar{n}_{\Omega}$, where

$$\bar{n}_{\Omega} = \frac{1}{\exp [\beta (E_{\Omega} + u'(\bar{n}) - \mu)] + \chi}.\quad (44)$$

Next, the entropy is given by

$$\begin{aligned}S &= - \frac{\partial \Phi}{\partial T} \Big|_{\mu,V}, \\ &= -V \frac{\partial u(\bar{n})}{\partial T} \Big|_{\mu,V} + \bar{N} \frac{\partial u'(\bar{n})}{\partial T} \Big|_{\mu,V} + u'(\bar{n}) \frac{\partial \bar{N}}{\partial T} \Big|_{\mu,V}\end{aligned}$$

$$\begin{aligned}
& + \chi \sum_{\Omega} \ln (1 + \chi \exp [-\beta (E_{\Omega} + u'(\bar{n}) - \mu)]) \\
& + \chi^2 T \sum_{\Omega} \frac{(E_{\Omega} + u'(\bar{n}) - \mu) \left(-\frac{d\beta}{dT} \right) - \beta \frac{\partial u'(\bar{n})}{\partial T} \Big|_{\mu, V}}{\exp [\beta (E_{\Omega} + u'(\bar{n}) - \mu)] + \chi},
\end{aligned} \tag{45}$$

or in a more compact form,

$$\begin{aligned}
S = & \chi \sum_{\Omega} \ln (1 + \chi \exp [-\beta (E_{\Omega} + u'(\bar{n}) - \mu)]) \\
& + \frac{1}{T} \sum_{\Omega} \bar{n}_{\Omega} (E_{\Omega} + u'(\bar{n}) - \mu).
\end{aligned} \tag{46}$$

Moreover, the mean energy reads

$$\begin{aligned}
\bar{E} = & \frac{\partial (\beta \Phi)}{\partial \beta} \Big|_{z, V}, \\
= & \frac{\partial}{\partial \beta} [\beta V u(\bar{n}) - \beta \bar{N} u'(\bar{n})] \Big|_{z, V} \\
& - \chi \sum_{\Omega} \frac{\chi z \exp [-\beta (E_{\Omega} + u'(\bar{n}))]}{1 + \chi z \exp [-\beta (E_{\Omega} + u'(\bar{n}))]} \left(-E_{\Omega} - \frac{\partial}{\partial \beta} [\beta u'(\bar{n})] \Big|_{z, V} \right), \\
= & U(V, \bar{n}) + \beta V \frac{\partial u(\bar{n})}{\partial \beta} \Big|_{z, V} - \bar{N} \frac{\partial [\beta u'(\bar{n})]}{\partial \beta} \Big|_{z, V} - \beta u'(\bar{n}) \frac{\partial \bar{N}}{\partial \beta} \Big|_{z, V} \\
& + \sum_{\Omega} \frac{E_{\Omega}}{z^{-1} \exp [\beta (E_{\Omega} + u'(\bar{n}))] + \chi} + \bar{N} \frac{\partial [\beta u'(\bar{n})]}{\partial \beta} \Big|_{z, V}.
\end{aligned} \tag{47}$$

After some algebraic manipulations, one can rewrite this expression as

$$\bar{E} = \sum_{\Omega} \bar{n}_{\Omega} E_{\Omega} + U(V, \bar{n}). \tag{48}$$

Finally, we derive the pressure

$$\begin{aligned}
p = & - \frac{\partial \Phi}{\partial V} \Big|_{\mu, T}, \\
= & -u(\bar{n}) + u'(\bar{n}) \frac{\partial \bar{N}}{\partial V} \Big|_{\mu, T} + \frac{\chi T}{V} \sum_{\Omega} \ln (1 + \chi \exp [-\beta (E_{\Omega} + u'(\bar{n}) - \mu)]), \\
= & -\frac{\Phi}{V},
\end{aligned} \tag{49}$$

where we have used the Eq. (43) and the fact that the particle density does not depend upon the volume. It is worth mentioning that such thermal functions were recently calculated in [83–85] for Lorentz-violating systems.

C. Analytical results for three-dimensional boxes

We exemplify our model constructed above with the example of the three-dimensional box. The respective spectral energy is

$$E_{\eta_x, \eta_y, \eta_z}^{\text{Box}} = \frac{\pi^2 \hbar^2}{2m} \left(\frac{\eta_x^2}{L_x^2} + \frac{\eta_y^2}{L_y^2} + \frac{\eta_z^2}{L_z^2} \right). \quad (50)$$

Here, the grand potential of an *interacting* gas is

$$\Phi = -k_B T \chi \sum_{\{\eta_x, \eta_y, \eta_z\}} \ln \left\{ 1 + \chi \exp \left[-\beta \left(E_{\eta_x, \eta_y, \eta_z}^{\text{Box}} + u'(\bar{n}) - \mu \right) \right] \right\} + U(V, \bar{n}) - u'(\bar{n}) \bar{N}. \quad (51)$$

To proceed further, the *Euler-MacLaurin formula* [21, 86] must be utilized,

$$\begin{aligned} \sum_n F(n) &= \int_0^\infty F(n) dn + \frac{1}{2} F(0) \\ &\quad - \frac{1}{2!} B_2 F'(0) - \frac{1}{4!} B_4 F'''(0) + \dots, \end{aligned} \quad (52)$$

which allows to perform the calculation in an exact form, namely

$$\begin{aligned} \Phi &= -k_B T \chi \int_0^\infty \int_0^\infty \int_0^\infty d\eta_x d\eta_y d\eta_z \ln \left\{ 1 + \chi \mathfrak{z} \exp \left[-\beta E_{\eta_x, \eta_y, \eta_z}^{\text{Box}} \right] \right\} \\ &\quad + \frac{k_B T \chi}{2} \int_0^\infty \int_0^\infty d\eta_y d\eta_z \ln \left\{ 1 + \chi \mathfrak{z} \exp \left[-\beta E_{0, \eta_y, \eta_z}^{\text{Box}} \right] \right\} \\ &\quad + \frac{k_B T \chi}{2} \int_0^\infty \int_0^\infty d\eta_x d\eta_z \ln \left\{ 1 + \chi \mathfrak{z} \exp \left[-\beta E_{\eta_x, 0, \eta_z}^{\text{Box}} \right] \right\} \\ &\quad + \frac{k_B T \chi}{2} \int_0^\infty \int_0^\infty d\eta_x d\eta_y \ln \left\{ 1 + \chi \mathfrak{z} \exp \left[-\beta E_{\eta_x, \eta_y, 0}^{\text{Box}} \right] \right\} \\ &\quad + \frac{k_B T \chi}{4} \int_0^\infty d\eta_x \ln \left\{ 1 + \chi \mathfrak{z} \exp \left[-\beta E_{\eta_x, 0, 0}^{\text{Box}} \right] \right\} \\ &\quad + \frac{k_B T \chi}{4} \int_0^\infty d\eta_y \ln \left\{ 1 + \chi \mathfrak{z} \exp \left[-\beta E_{0, \eta_y, 0}^{\text{Box}} \right] \right\} \\ &\quad + \frac{k_B T \chi}{4} \int_0^\infty d\eta_z \ln \left\{ 1 + \chi \mathfrak{z} \exp \left[-\beta E_{0, 0, \eta_z}^{\text{Box}} \right] \right\} \\ &\quad + \frac{k_B T \chi}{8} \ln(1 + \chi \mathfrak{z}) + U(V, \bar{n}) - u'(\bar{n}) \bar{N}, \end{aligned} \quad (53)$$

where we have defined $\mathfrak{z} = ze^{-\beta u'(\bar{n})}$. After performing the integrals, we obtain

$$\Phi = \frac{\mathcal{V}}{\lambda^3} h_{\frac{5}{2}}(\mathfrak{z}) - \frac{1}{4} \frac{\mathcal{S}}{\lambda^2} h_2(\mathfrak{z}) + \frac{1}{16} \frac{\mathcal{L}}{\lambda} h_{\frac{3}{2}}(\mathfrak{z}) - \frac{1}{8} h_1(\mathfrak{z}) + U(V, \bar{n}) - u'(\bar{n}) \bar{N}, \quad (54)$$

where $\lambda = h/\sqrt{2\pi mk_B T}$ is the thermal wavelength, $\mathcal{V} = L_x L_y L_z$ is the volume, $\mathcal{S} = 2(L_x L_y + L_y L_z + L_z L_x)$ the area of the surface, $\mathcal{L} = 4(L_x + L_y + L_z)$ the total length of

the side of the box and

$$h_\sigma(\mathfrak{z}) = \frac{1}{\Gamma(\sigma)} \int_0^\infty \frac{t^{\sigma-1}}{\mathfrak{z}^{-1}e^t + \chi} dt = \begin{cases} f_\sigma(\mathfrak{z}), & \text{for fermions } (\chi = 1) \\ g_\sigma(\mathfrak{z}), & \text{for bosons } (\chi = -1) \end{cases}. \quad (55)$$

The boundary effects in Eq. (54) are represented by the second and third terms which are proportional to the perimeter \mathcal{L} and the surface \mathcal{S} term. We should notice that these terms are modified by the interaction term $u'(\bar{n})$. Also, we can carry out a similar calculation involving a two-dimensional box. Here, a straightforward question naturally arises: how are thermal properties are influenced if one considers spherical (1), cylindrical (2), ellipsoidal (3) and toroidal (4) potentials instead? Despite being an intriguing question, such analysis cannot be performed analytically. Looking towards to this direction, such analysis will be performed numerically in an upcoming work.

D. Analytical results for angular constraints

The exact solutions for *interacting* gases in angular constraints can also be calculated with the help of the *Euler-MacLaurin* formula. Here, we consider an *interacting* quantum gas confined in an one-dimensional ring of the radius R . The energy of the particle in such an angular scenario is determined by periodic boundary conditions:

$$E_\eta = \frac{\hbar^2}{2mR^2} \eta^2. \quad (56)$$

The grand potential for this case is given by

$$\begin{aligned} \Phi &= -k_B T \chi \sum_{\eta=-\infty}^{\infty} \ln \left\{ 1 + \chi \mathfrak{z} \exp \left[-\frac{\beta \hbar^2}{2mR^2} \eta^2 \right] \right\} + U(V, \bar{n}) - u'(\bar{n}) \bar{N}, \\ &= -2k_B T \chi \sum_{\eta=0}^{\infty} \ln \left\{ 1 + \chi \mathfrak{z} \exp \left[-\frac{\beta \hbar^2}{2mR^2} \eta^2 \right] \right\} - k_B T \chi \ln \{1 + \chi \mathfrak{z}\} + U(V, \bar{n}) - u'(\bar{n}) \bar{N}. \end{aligned} \quad (57)$$

The summation over the discrete parameter η can be converted into an integral which leads to

$$\Phi = \frac{\mathcal{L}}{\lambda} h_{\frac{3}{2}}(\mathfrak{z}) - h_1(\mathfrak{z}) + U(V, \bar{n}) - u'(\bar{n}) \bar{N}. \quad (58)$$

where $\mathcal{L} = 2\pi R$ and $h_\sigma(\mathfrak{z})$ is the interaction. We can also notice that there is no boundary effect here. Notably, we could use these results to study the thermodynamic properties of a conducting ring and other similar systems. Moreover, if one does not consider the interactions, the results presented in subsections VII C and VII D reproduce those encountered in Ref. [17].

E. Analytical results for the torus

We can proceed as before to get an exact solution for the torus. The grand potential for this case is given by

$$\begin{aligned}\Phi &= -T\chi \sum_{\delta=-\infty}^{\infty} \ln \left\{ 1 + \chi \mathfrak{z} \exp \left[-\frac{\beta \hbar^2 F(\alpha, \eta)}{2ma^2 p^2} \delta^2 \right] \right\} + U(V, \bar{n}) - u'(\bar{n}) \bar{N}, \\ &= -2T\chi \sum_{\delta=1}^{\infty} \ln \left\{ 1 + \chi \mathfrak{z} \exp \left[-\frac{\beta \hbar^2 F(\alpha, \eta)}{2ma^2 p^2} \delta^2 \right] \right\} - T\chi \ln \{1 + \chi \mathfrak{z}\} + U(V, \bar{n}) - u'(\bar{n}) \bar{N}.\end{aligned}\tag{59}$$

The summation over the discrete parameter δ can be rewritten as an integral, leading to

$$\Phi = \frac{ap^2}{F(\alpha, \eta)} \frac{\mathcal{L}}{\lambda} h_{\frac{3}{2}}(\mathfrak{z}) - h_1(\mathfrak{z}) + U(V, \bar{n}) - u'(\bar{n}) \bar{N}.\tag{60}$$

where $\mathcal{L} = 2\pi a$ and again the interaction is also present in the $h_\sigma(\mathfrak{z})$ function. We can also notice here that there is no boundary for the same reason as in the ring and that the final result is modified by a topological function $F(\alpha, \eta)$.

VIII. CONCLUSION AND FUTURE PERSPECTIVES

We examined the behavior of the thermodynamic functions for different geometries, i.e., spherical, cylindrical, ellipsoidal and toroidal ones; we primarily used the canonical ensemble for spinless particles. Moreover, *non-interacting* gases were also taken into account for the same geometries with the usage of the grand canonical ensemble description. The comparison of how geometry affected the system for spinless, fermions and bosons was provided as well. Moreover, two applications were given to corroborate our results: *Bose-Einstein condensate* and *helium dimer*. Furthermore, for the bosonic sector, independently of the geometry, the entropy and internal energy turned out to be greater than fermionic case; a standard configuration repeatedly happened for both of them, namely, *Ellipsoid > Cylinder > Sphere*. Also, it is worth mentioning that, for the toroidal case, there was an “inversion point” due to the winding number at $3k$. Thereby, we saw a modification in the thermal properties due to the topological parameter α . Finally, we constructed a model to provide the calculations of *interacting* quantum gases; it was implemented for three different cases: a cubical box, a ring and a torus. Such an interaction sector turned out to be more prominent since all results were derived analytically.

Another promising aspect to be investigated in condensed matter physics, is the thermal properties of anisotropic systems (with or without considering Lorentz violation). Such anisotropy may reveal new phenomena which can be confronted with experimental physics afterwards. In the case of phosphorene, one can assume electrons to have an anisotropic effective mass [87], which raises many possibilities: if we confine these electrons in a box, collisions with the walls will depend on the angle that the wall makes with anisotropy direction. More so, phonons behave likewise in such systems.

Acknowledgments

The authors would like to thank João Milton, Andrey Chaves, Diego Rabelo, Ewerthon Wagner and Paulo Porfírio for the fruitful suggestions during the preparation of this manuscript and Albert Petrov and Izeldin Ahmed for the careful reading of this work. Particularly, A. A. Araújo Filho acknowledges the Facultad de Física - Universitat de València

and Gonzalo J. Olmo for the kind hospitality when part of this work was made. Moreover, this work was partially supported by Conselho Nacional de Desenvolvimento Científico e Tecnológico (CNPq) - 142412/2018-0, Coordenação de Aperfeiçoamento de Pessoal de Nível Superior (CAPES) - Finance Code 001, and CAPES-PRINT (PRINT - PROGRAMA INSTITUCIONAL DE INTERNACIONALIZAÇÃO) - 88887.508184/2020-00.

- [1] D. R. Gaskell and D. E. Laughlin, *Introduction to the Thermodynamics of Materials* (CRC press, 2017).
- [2] R. DeHoff, *Thermodynamics in materials science* (CRC Press, 2006).
- [3] B. Mühlischlegel, D. Scalapino, and R. Denton, *Physical Review B* **6**, 1767 (1972).
- [4] J. W. Tester, M. Modell, *et al.*, *Thermodynamics and its Applications* (Prentice Hall PTR, 1997).
- [5] C. Lee, W. Yang, and R. G. Parr, *Physical Review B* **37**, 785 (1988).
- [6] A. A. Araújo-Filho, F. L. Silva, A. Righi, M. B. da Silva, B. P. Silva, E. W. S. Caetano, and V. N. Freire, *Journal of Solid State Chemistry* **250**, 68 (2017).
- [7] M. E. Casida, C. Jamorski, K. C. Casida, and D. R. Salahub, *The Journal of Chemical Physics* **108**, 4439 (1998).
- [8] M. D. Segall, P. J. D. Lindan, M. J. a. Probert, C. J. Pickard, P. J. Hasnip, S. Clark, and M. Payne, *Journal of Physics: Condensed Matter* **14**, 2717 (2002).
- [9] D. C. Langreth and M. J. Mehl, *Physical Review B* **28**, 1809 (1983).
- [10] F. L. R. Silva, A. A. A. Filho, M. B. da Silva, K. Balzuweit, J.-L. Bantignies, E. W. S. Caetano, R. L. Moreira, V. N. Freire, and A. Righi, *Journal of Raman Spectroscopy* **49**, 538 (2018).
- [11] A. Imanian and M. Modarres, *Proceedings of the Institution of Mechanical Engineers, Part O: Journal of Risk and Reliability* **230**, 598 (2016).
- [12] F. Reif, *Fundamentals of statistical and thermal physics* (Waveland Press, 2009).
- [13] A. A. Balandin, *Nature Materials* **10**, 569 (2011).
- [14] A. Bejan, *Advanced engineering thermodynamics* (John Wiley & Sons, 2016).
- [15] H. Potempa and L. Schweitzer, *Journal of Physics: Condensed Matter* **10**, L431 (1998).
- [16] W.-S. Dai and M. Xie, *Physics Letters A* **311**, 340 (2003).
- [17] W.-S. Dai and M. Xie, *Physical Review E* **70**, 016103 (2004).

- [18] L. Angelani, L. Casetti, M. Pettini, G. Ruocco, and F. Zamponi, Physical Review E **71**, 036152 (2005).
- [19] D. Braun, G. Montambaux, and M. Pascaud, Physical Review Letters **81**, 1062 (1998).
- [20] V. E. Kravtsov and V. I. Yudson, Physical Review Letters **82**, 157 (1999).
- [21] R. R. Oliveira, A. A. Araújo Filho, F. C. Lima, R. V. Maluf, and C. A. Almeida, The European Physical Journal Plus **134**, 495 (2019).
- [22] R. R. S. Oliveira, A. A. Araújo Filho, R. V. Maluf, and C. A. S. Almeida, Journal of Physics A: Mathematical and Theoretical **53**, 045304 (2020).
- [23] R. K. Pathria, *Statistical mechanics*, Vol. 45 (Pergamon, 1972).
- [24] L. D. Landau and E. M. Lifshitz, *Statistical Physics: Volume 5*, Vol. 5 (Elsevier, 2013).
- [25] N. Zettili, “Quantum mechanics: concepts and applications,” (2003).
- [26] H. Weyl, *Gesammelte Abhandlungen: Band 1 bis 4*, Vol. 4 (Springer-Verlag, 1968).
- [27] D. J. Griffiths and D. F. Schroeter, *Introduction to quantum mechanics* (Cambridge University Press, 2018).
- [28] T. Kereselidze, T. Tchelidze, T. Nadareishvili, and R. Y. Kezerashvili, Physica E: Low-dimensional Systems and Nanostructures **81**, 196 (2016).
- [29] P. A. M. Dirac, *Lectures on quantum mechanics*, Vol. 2 (Courier Corporation, 2001).
- [30] G. E. Andrews, R. Askey, and R. Roy, *Special functions*, Vol. 71 (Cambridge university press, 1999).
- [31] R. A. Silverman *et al.*, *Special functions and their applications* (Courier Corporation, 1972).
- [32] W. W. Bell, *Special functions for scientists and engineers* (Courier Corporation, 2004).
- [33] H. Krivine, Nuclear Physics A **457**, 125 (1986).
- [34] A. Chaves and D. Neilson, “Two-dimensional semiconductors host high-temperature exotic state,” (2019).
- [35] L. V. Butov, C. W. Lai, A. L. Ivanov, A. C. Gossard, and D. S. Chemla, Nature **417**, 47 (2002).
- [36] Z. Wang, D. A. Rhodes, K. Watanabe, T. Taniguchi, J. C. Hone, J. Shan, and K. F. Mak, Nature **574**, 76 (2019).
- [37] G. W. Burg, N. Prasad, K. Kim, T. Taniguchi, K. Watanabe, A. H. MacDonald, L. F. Register, and E. Tutuc, Physical Review Letters **120**, 177702 (2018).
- [38] S. Chen and P. Tartaglia, Optics Communications **6**, 119 (1972).

[39] V. Degtyarev, S. Khazanova, and N. Demarina, *Scientific Reports* **7**, 1 (2017).

[40] L. Bürgi, N. Knorr, H. Brune, M. A. Schneider, and K. Kern, *Applied Physics A* **75**, 141 (2002).

[41] H. Lee, N. Campbell, J. Lee, T. Asel, T. Paudel, H. Zhou, J. Lee, B. Noesges, J. Seo, B. Park, *et al.*, *Nature materials* **17**, 231 (2018).

[42] R. Weill, A. Bekker, B. Levit, M. Zhurahov, and B. Fischer, *Optics Express* **25**, 18963 (2017).

[43] X. Liu, J. Zhang, Z. Zhang, X. Lin, Y. Yu, X. Xing, Z. Jin, Z. Cheng, and G. Ma, *Applied Physics Letters* **111**, 152906 (2017).

[44] C.-X. Zhang, S.-G. Peng, and K. Jiang, *Physical Review A* **98**, 043619 (2018).

[45] V. V. Romanov, N. T. Bagraev, V. A. Kozhevnikov, and G. K. Sizykh, in *Journal of Physics: Conference Series*, Vol. 1236 (IOP Publishing, 2019) p. 012014.

[46] D. A. Baghdasaryan, D. B. Hayrapetyan, E. M. Kazaryan, and H. A. Sarkisyan, *Physica E: Low-Dimensional Systems and Nanostructures* **101**, 1 (2018).

[47] M. Däne and A. Gonis, *Computation* **4**, 24 (2016).

[48] S. Jungblut, J.-O. Joswig, and A. Eychmüller, *Physical Chemistry Chemical Physics* **21**, 5723 (2019).

[49] R. Kutner, *Physics Letters A* **81**, 239 (1981).

[50] M. Ligare, *American Journal of Physics* **78**, 815 (2010).

[51] M. Wilkens and C. Weiss, *Journal of Modern Optics* **44**, 1801 (1997).

[52] H. Pajkowski and R. Pathria, *Journal of Physics A: Mathematical and General* **10**, 561 (1977).

[53] P. Freyd, D. Yetter, J. Hoste, W. R. Lickorish, K. Millett, and A. Ocneanu, *Bulletin of the American Mathematical Society* **12**, 239 (1985).

[54] A. Gangopadhyaya, J. V. Mallow, C. Rasinariu, and J. Bougie, preprint arXiv:2005.06683 (2020).

[55] J. Benbourenane and H. Eleuch, *Results in Physics* , 103034 (2020).

[56] E. Anderson, *Classical and Quantum Gravity* **26**, 135021 (2009).

[57] K. A. Mitchell, *Physical Review A* **63**, 042112 (2001).

[58] Z. Gong, N. Yoshioka, N. Shibata, and R. Hamazaki, *Physical Review A* **101**, 052122 (2020).

[59] J. Wachsmuth and S. Teufel, *Physical Review A* **82**, 022112 (2010).

[60] D. Biswas and S. Ghosh, preprint arXiv:1908.06423 (2019).

[61] H.-F. Zhang, C.-M. Wang, and L.-S. Wang, *Nano Letters* **2**, 941 (2002).

[62] S. Xu, Z. Yan, K.-I. Jang, W. Huang, H. Fu, J. Kim, Z. Wei, M. Flavin, J. McCracken, R. Wang, *et al.*, *Science* **347**, 154 (2015).

[63] P. Freyd, D. Yetter, J. Hoste, W. R. Lickorish, K. Millett, and A. Ocneanu, *Bulletin of the American Mathematical Society* **12**, 239 (1985).

[64] E. Witten, *Communications in Mathematical Physics* **121**, 351 (1989).

[65] E. Witten, *Communications in Mathematical Physics* **117**, 353 (1988).

[66] H. N. Temperley and E. H. Lieb, *Proceedings of the Royal Society of London. A. Mathematical and Physical Sciences* **322**, 251 (1971).

[67] D. Sumners, in *Proceedings of Symposia in Applied Mathematics*, Vol. 45 (1992) pp. 39–72.

[68] M. Bodner, J. Patera, and M. Peterson, *Journal of Mathematical Physics* **53**, 013516 (2012).

[69] W.-y. Qiu and H.-w. Xin, *Journal of Molecular Structure: THEOCHEM* **429**, 81 (1998).

[70] J. Tompkins, Rose-hulman. edu (2005).

[71] W.-y. Qiu and H.-w. Xin, *Journal of Molecular Structure: THEOCHEM* **429**, 81 (1998).

[72] J. R. Munkres, *Elements of algebraic topology* (CRC Press, 2018).

[73] S. Kilić, E. Krotscheck, and R. Zillich, *Journal of Low Temperature Physics* **116**, 245 (1999).

[74] S. Kilić, E. Krotscheck, and L. Vranješ, *Journal of Low Temperature Physics* **119**, 715 (2000).

[75] W. M. Gersbacher and F. J. Milford, *Journal of Low Temperature Physics* **9**, 189 (1972).

[76] E. Zaremba and W. Kohn, *Physical Review B* **15**, 1769 (1977).

[77] M. Bretz and J. G. Dash, *Physical Review Letters* **26**, 963 (1971).

[78] M. Bretz and J. G. Dash, *Physical Review Letters* **27**, 647 (1971).

[79] M. S. Dresselhaus, G. Dresselhaus, P. C. Eklund, and A. M. Rao, in *The physics of fullerene-based and fullerene-related materials* (Springer, 2000) pp. 331–379.

[80] A. Jorio, G. Dresselhaus, and M. S. Dresselhaus, *Carbon nanotubes: advanced topics in the synthesis, structure, properties and applications*, Vol. 111 (Springer Science & Business Media, 2007).

[81] M. Saarela, B. E. Clements, E. Krotscheck, and F. V. Kusmartsev, *Journal of Low Temperature Physics* **93**, 971 (1993).

[82] M. Saarela and F. V. Kusmartsev, *Physics Letters A* **202**, 317 (1995).

[83] J. A. A. S. Reis *et al.*, preprint arXiv:2005.11453 (2020).

[84] A. A. Filho, Araújo, preprint arXiv:2004.07799 (2020).

[85] R. V. Maluf *et al.*, preprint arXiv:2003.02380 (2020).

- [86] R. Oliveira and A. Araújo Filho, The European Physical Journal Plus **135**, 99 (2020).
- [87] S. M. Cunha, D. R. da Costa, L. C. Felix, A. Chaves, and J. M. Pereira Jr, Physical Review B **102**, 045427 (2020).